Surface Frontogenesis in Isentropic Coordinates

SCOTT R. FULTON

Department of Mathematics and Computer Science, Clarkson University, Potsdam, New York

WAYNE H. SCHUBERT

Department of Atmospheric Science, Colorado State University, Fort Collins, Colorado

(Manuscript received 27 August 1990, in final form 20 May 1991)

ABSTRACT

The semigeostrophic equations take a particularly simple form when isentropic and geostrophic coordinates are used simultaneously: the horizontal ageostrophic velocities are entirely implicit, and the entire dynamics reduces to a predictive equation for the potential pseudodensity (inverse Ertel potential vorticity) and an invertibility relation. However, a perceived disadvantage of isentropic coordinates is the difficulty of treating a lower boundary that is not an isentropic surface.

Here we present the massless layer method, which allows isentropic surfaces to intersect the lower boundary, and show that this extends the applicability of potential vorticity modeling in isentropic/geostrophic coordinates. When applied to the classic problem of surface frontogenesis by a vertically independent deformation field, the model produces realistic fronts with a surface discontinuity in finite time and tropopause folding, without the need for special treatment of the lower boundary.

1. Introduction

An emerging view in atmospheric dynamics is that the simplest way to diagnose or predict balanced flows is through the use of the Rossby–Ertel potential vorticity on isentropic surfaces. This is sometimes referred to as "IPV thinking" or "IPV modeling." While it is true that the use of isentropic coordinates and the Rossby–Ertel potential vorticity dates back about fifty years (Rossby 1937, 1940; Montgomery 1937; Ertel 1942), the modern view has added much—most notably the concepts of balance, invertibility, and transformed horizontal coordinates. The acceptance of the modern view is in large part due to the illuminating discussion of Hoskins et al. (1985), who point out that it involves two main mathematical principles—the potential vorticity conservation principle as the prediction equation and the invertibility principle as the diagnostic equation to obtain the balanced wind and mass fields from the potential vorticity field. Hoskins et al. then proceed to show how IPV thinking can lead to increased insight into such phenomena as the formation of cutoff cyclones and blocking anticyclones, Rossby wave propagation, and baroclinic/barotropic instability.

Corresponding author address: Dr. Scott R. Fulton, Dept. of Mathematics and Computer Science, Clarkson University, Potsdam, NY 13699-5815.

An important advantage to be exploited in the present work is that which is gained by using IPV modeling in conjunction with certain horizontal coordinate transformations (McWilliams and Gent 1980; Buzzi et al. 1981). This advantage is gained when the IPV approach is used with a filtered model that includes horizontal advection by the ageostrophic or divergent part of the wind. In such situations the proper choice of transformed horizontal coordinates can make this ageostrophic or divergent advection entirely implicit, eliminating the need to solve an additional elliptic equation. We have recently shown that this is a useful way to examine flows generated by groups of convective clouds, for example, the development of tropical cyclones (Schubert and Alworth 1987), the balanced atmospheric response to squall lines (Schubert et al. 1989), and the generation of zonal rotational flow by the convection of the ITCZ (Schubert et al. 1991). These studies all use the isentropic coordinate in the vertical and a vortex coordinate in the horizontal (potential radius for tropical cyclones, the geostrophic coordinate for squall lines, and potential latitude for the Hadley cirulation). An apparent limitation of all these studies is that they present results in which the lower boundary is assumed to be an isentropic surface. How do we handle situations where the lower boundary is not an isentropic surface? There seems to be a fairly widespread belief that this is very inconvenient

or perhaps even impossible. The simplest prototype problem to treat in this regard is probably the classic problem of surface frontogenesis by a vertically independent deformation field. Thus, if the emerging technique of IPV modeling is to be further advanced, we should demonstrate that it can handle surface frontogenesis in a convenient and accurate fashion.

This paper is organized as follows. Section 2 reviews the semigeostrophic equations in isentropic coordinates, and the invertibility principle in geostrophic space is derived in section 3. In section 4 we show how to extend the semigeostrophic equations to the case where the lower boundary is not an isentropic surface by incorporating a massless layer. The equations developed are then used to solve the classic two-dimensional frontogenesis problem in section 5, and concluding remarks are given in section 6.

2. Semigeostrophic theory and the potential pseudodensity equation

We begin with the f-plane system of equations with the geostrophic momentum approximation (Eliassen 1948; Hoskins 1975) and proceed with an analysis similar to that of Schubert et al. (1989). Assuming the flow is frictionless and adiabatic, and using potential temperature as the vertical coordinate, our system becomes

$$\frac{Du_g}{Dt} - fv + \frac{\partial M}{\partial x} = 0, \tag{2.1}$$

$$\frac{Dv_g}{Dt} + fu + \frac{\partial M}{\partial y} = 0, \tag{2.2}$$

$$\frac{\partial M}{\partial \theta} = \Pi, \tag{2.3}$$

$$\frac{D\sigma}{Dt} + \sigma\left(\frac{\partial u}{\partial x} + \frac{\partial v}{\partial y}\right) = 0, \tag{2.4}$$

where

$$(u_g, v_g) = \frac{1}{f}\left(-\frac{\partial M}{\partial y}, \frac{\partial M}{\partial x}\right) \tag{2.5}$$

are the components of geostrophic velocity, (u, v) the horizontal components of the total velocity, $\Pi = c_p (p/p_0)^\kappa$ the Exner function, $M = \theta\Pi + \phi$ the Montgomery potential with ϕ the geopotential, $\sigma = -\partial p/\partial\theta$ the pseudodensity, and

$$\frac{D}{Dt} = \frac{\partial}{\partial t} + u\frac{\partial}{\partial x} + v\frac{\partial}{\partial y} \tag{2.6}$$

the total derivative.

By combining x and y partial derivatives of (2.1) and (2.2) one can derive the equation

$$\frac{D\zeta}{Dt} + \zeta\left(\frac{\partial u}{\partial x} + \frac{\partial v}{\partial y}\right) = 0, \tag{2.7}$$

for the quantity

$$\zeta = f + \frac{\partial v_g}{\partial x} - \frac{\partial u_g}{\partial y} + \frac{1}{f}\frac{\partial(u_g, v_g)}{\partial(x, y)}, \tag{2.8}$$

which we refer to as the isentropic absolute vorticity, in view of (2.7). We can eliminate the isentropic divergence between (2.4) and (2.7) to obtain

$$\frac{D\sigma^*}{Dt} = 0, \tag{2.9}$$

where

$$\sigma^* = \frac{f}{\zeta}\sigma \tag{2.10}$$

is the potential pseudodensity. According to (2.10) the potential pseudodensity involves the wind field ζ and the mass field σ. Since ζ can be expressed in terms of u_g and v_g and hence M through geostrophic balance (2.5), and since σ can be expressed in terms of Π and hence M through hydrostatic balance (2.3), there exists a second-order partial differential equation relating M and σ^*. This equation, along with its associated boundary conditions, is usually referred to as the invertibility principle. Thus, we have (2.9) as a predictive equation for σ^* and an associated invertibility principle from which we can diagnose M from a known σ^*. However, when D/Dt is expressed in physical space by (2.6), (2.9) involves advection by the total wind, in which case the predictive equation for σ^* and the invertibility principle do not form a closed system. This is the point at which geostrophic coordinates $(X, Y, \Theta, T) = (x + v_g/f, y - u_g/f, \theta, t)$ enter the picture. The transformation to geostrophic coordinates makes the horizontal advecting velocity geostrophic, so that (2.9) becomes

$$\frac{\partial\sigma^*}{\partial T} + u_g\frac{\partial\sigma^*}{\partial X} + v_g\frac{\partial\sigma^*}{\partial Y} = 0, \tag{2.11}$$

which is the fundamental predictive equation of the model. Because the prediction of σ^* is then performed in geostrophic coordinate space, the invertibility principle must also be formulated in this space.

3. Invertibility principle in geostrophic space

Introducing the Bernoulli function $M^* = M + \frac{1}{2}(u_g^2 + v_g^2)$, it can be shown that the geostrophic and hydrostatic relations in (X, Y, Θ) take the form

$$(fv_g, -fu_g, \Pi) = \left(\frac{\partial M^*}{\partial X}, \frac{\partial M^*}{\partial Y}, \frac{\partial M^*}{\partial \Theta}\right), \quad (3.1)$$

which is identical to the form taken in (x, y, θ). Also, the isentropic vorticity in (X, Y, Θ) takes the form

$$\frac{f}{\zeta} = \frac{\partial(x, y)}{\partial(X, Y)} = 1 - \frac{1}{f}\left(\frac{\partial v_g}{\partial X} - \frac{\partial u_g}{\partial Y}\right) + \frac{1}{f^2}\frac{\partial(u_g, v_g)}{\partial(X, Y)}. \quad (3.2)$$

Thus, σ^* depends only on M^*, and we again conclude that the wind and mass fields can in principle be obtained from σ^* if we can somehow invert it to obtain M^*.

The relation between M^* and σ^* is derived as follows. From the definition of σ^* and (3.2) we have

$$\frac{\partial(x, y, \Pi)}{\partial(X, Y, \Theta)} + \Gamma\sigma^* = 0, \quad (3.3)$$

where $\Gamma = d\Pi/dp = \kappa\Pi/p$. Expressing x and y in terms of u_g and v_g, and then using (3.1), we can write (3.3) as

$$\frac{1}{f^4}\begin{vmatrix} \frac{\partial^2 M^*}{\partial X^2} - f^2 & \frac{\partial^2 M^*}{\partial Y \partial X} & \frac{\partial^2 M^*}{\partial \Theta \partial X} \\ \frac{\partial^2 M^*}{\partial X \partial Y} & \frac{\partial^2 M^*}{\partial Y^2} - f^2 & \frac{\partial^2 M^*}{\partial \Theta \partial Y} \\ \frac{\partial^2 M^*}{\partial X \partial \Theta} & \frac{\partial^2 M^*}{\partial Y \partial \Theta} & \frac{\partial^2 M^*}{\partial \Theta^2} \end{vmatrix} + \Gamma\sigma^* = 0. \quad (3.4a)$$

If the upper boundary is an isentropic surface with potential temperature Θ_T and the Exner function Π_T—or equivalently the pressure p_T—is specified there (e.g., constant for an isobaric top), the upper boundary condition for (3.4a) is simply

$$\frac{\partial M^*}{\partial \Theta} = \Pi_T \quad \text{at} \quad \Theta = \Theta_T. \quad (3.4b)$$

Likewise, if the lower boundary is the isentropic surface $\Theta = \Theta_B$ and the surface geopotential ϕ_S is specified there (e.g., $\phi_S = 0$ for a flat lower boundary), then $M = \Theta\Pi + \phi_S$ at $\Theta = \Theta_B$. Written in terms of M^*, this lower boundary condition becomes

$$M^* - \Theta\frac{\partial M^*}{\partial \Theta} - \frac{1}{2f^2}\left[\left(\frac{\partial M^*}{\partial X}\right)^2 + \left(\frac{\partial M^*}{\partial Y}\right)^2\right] = \phi_S \quad \text{at} \quad \Theta = \Theta_B. \quad (3.4c)$$

Together with appropriate lateral boundary conditions, Eqs. (2.11), (3.1), and (3.4) form a closed system. The computational scheme is as follows: knowing σ^*, solve (3.4) for M^*; use (3.1) to compute u_g and v_g; use these geostrophic winds in (2.11) to predict a new σ^*. However, to make the system useful for modeling realistic flows we must relax the assumption of an isentropic lower boundary.

4. The massless layer approach

To apply the semigeostrophic equations when the lower boundary is not necessarily an isentropic surface, we adopt an approach that has proved useful in such contexts as the definition of available potential energy (Lorenz 1955), the analysis of baroclinic instability (Bretherton 1966; Hoskins et al. 1985; James and Hoskins 1985; Hsu and Arakawa 1990), and the finite-amplitude Eliassen–Palm theorem (Andrews 1983). The key idea is to think of an isentropic surface that intersects the earth's surface as continuing just under the earth's surface with a pressure equal to the surface pressure. At any horizontal position where two distinct isentropic surfaces run just under the earth's surface (and hence have the same pressure), there is no mass trapped between them, so that $\sigma^* = \sigma = 0$ there. This "massless layer" approach is consistent with Bretherton's (1966) conclusion that "any flow with potential temperature variations over a horizontal rigid plane boundary may be considered equivalent to a flow without such variations, but with a concentration of potential vorticity very close to the boundary." We have simply replaced Bretherton's thin sheet of infinite potential vorticity with a thin sheet of zero potential pseudodensity.

We extend the semigeostrophic equations to the massless layer as follows. Following Andrews (1983), we let the surface geopotential and potential temperature be given by $\phi_S(x, y, t)$ and $\theta_S(x, y, t)$, respectively, so that

$$\phi(x, y, \theta_S(x, y, t), t) = \phi_S(x, y, t), \quad (4.1)$$

and define ϕ and p for $\theta < \theta_S$ by

$$\phi(x, y, \theta, t) = \phi_S(x, y, t), \quad p(x, y, \theta, t) = p_S(x, y, t) \equiv p(x, y, \theta_S, t). \quad (4.2)$$

From the definitions of σ, Π, and M we then obtain

$$\sigma = 0, \quad \Pi = \Pi_S \equiv \Pi(p_S), \quad M = \theta\Pi_S + \phi_S \quad (4.3)$$

for $\theta < \theta_S$. We note that p, Π, and M are

continuous at $\theta = \theta_S$, but σ jumps discontinuously from $\sigma = 0$ for $\theta < \theta_S$ to $\sigma > 0$ for $\theta > \theta_S$. Also, p and Π are constant in the massless layer, while M varies linearly with θ there. From (4.3) we see that the hydrostatic relation (2.3) holds for $\theta < \theta_S$; a careful analysis (see Appendix) shows that it also holds at $\theta = \theta_S$. Then defining (u_g, v_g) for $\theta < \theta_S$ by (2.5) and defining (u, v) so that (2.1) and (2.2) hold in the massless layer completes the extension of semigeostrophic theory. Since the governing equations and definitions all apply unchanged in the massless layer, the derivation of the potential pseudodensity equation, the transformation to geostrophic coordinates, and the derivation of the invertibility principle all proceed exactly as in sections 2 and 3.

We thus conclude that (2.11), (3.1), and (3.4) are valid in the massless layer. The lower boundary condition (3.4c) is in fact valid anywhere that $\Theta_B \leq \Theta_S$ holds; for convenience, we choose a constant value Θ_B that satisfies this constraint everywhere and apply (3.4c) at Θ_B rather than at Θ_S. We then predict the evolution of the entire σ^* field (including the zero potential pseudodensity region) with (2.11). Of course, $\sigma^* = 0$ in the massless layer, but the boundary of the region may move. Since this boundary is the surface potential temperature, that is, that value of Θ at which σ^* jumps from zero to a positive value, this procedure also predicts Θ_S. Any numerical method used to solve (2.11) must cope properly with the discontinuity in σ^* at Θ_S. However, workable schemes do exist. For example, recently Arakawa and Hsu (1990), in the context of solving (2.4) in a primitive equation model, have proposed a finite- difference scheme that has very small dissipation and computational dispersion and guarantees positive definiteness. Note, however, that the discontinuity in σ^* presents less of a problem in solving (3.4) numerically, since σ^* plays the role of the forcing, rather than the solution, and is not differentiated.

5. Frontogenesis by horizontal deformation fields

Let us now reconsider the two-dimensional frontogenesis problem of Hoskins (1971, 1972) and Hoskins and Bretherton (1972). Fronts oriented in the y direction are assumed to be forced by a pure deformation field so that

$$u_g(x, y, \theta, t) = -\alpha x, \tag{5.1a}$$

$$v_g(x, y, \theta, t) = \alpha y + v_g'(x, \theta, t), \tag{5.1b}$$

with the first terms on the right-hand side representing the fixed (or "slowly" varying) deformation field and the v_g' term representing the rotational flow generated during the frontogenesis. Assuming σ^* is independent of y so that

$$\frac{\partial \sigma^*}{\partial y} = \frac{\partial X}{\partial y}\frac{\partial \sigma^*}{\partial X} + \frac{\partial Y}{\partial y}\frac{\partial \sigma^*}{\partial Y} = 0, \tag{5.2}$$

and using the definitions of (X, Y) and the assumptions (5.1), we obtain

$$\frac{\partial \sigma^*}{\partial Y} = -\frac{\alpha}{f}\frac{\partial \sigma^*}{\partial X}. \tag{5.3}$$

Using this result in (2.11), we obtain

$$\frac{\partial \sigma^*}{\partial T} - \alpha X \frac{\partial \sigma^*}{\partial X} = 0. \tag{5.4}$$

The solution of (5.4) is given by

$$\sigma^*(X, \Theta, T) = \sigma^*(Xe^{\alpha T}, \Theta, 0). \tag{5.5}$$

For the initial condition we assume that σ^* takes on the constant value σ_T in the top part, the larger constant value σ_B in the bottom part, and a zero value in the massless region of the model atmosphere. These three regions are separated by the tropopause interface potential temperature $\theta_I(x)$ and the surface potential temperature $\theta_S(x)$. To allow the possibility of smoothing discontinuous jumps in σ^* over small ranges specified by $\Delta\theta_S$ and $\Delta\theta_I$ we set

$$\sigma^*(x, \theta, 0) = \frac{1}{2}\left[\sigma_T + \sigma_B \tanh\left(\frac{\theta - \theta_S}{\Delta\theta_S}\right) - (\sigma_B - \sigma_T)\tanh\left(\frac{\theta - \theta_I}{\Delta\theta_I}\right)\right], \tag{5.6}$$

which reduces to

$$\sigma^*(x, \theta, 0) = \begin{cases} \sigma_T, & \theta_I(x,0) < \theta \leq \theta_T \\ \sigma_B, & \theta_S(x,0) < \theta < \theta_I(x,0) \\ 0, & \theta_B \leq \theta < \theta_S(x,0) \end{cases} \tag{5.7}$$

in the limit as $\Delta\theta_S \to 0$ and $\Delta\theta_I \to 0$. If the x derivatives of $\theta_S(x,0)$ and $\theta_I(x,0)$ are sufficiently small, the relative vorticity associated with this initial σ^* field will be much less than f and σ^* will approximately equal σ. Then we can integrate (5.6) from θ_B to θ_T to obtain

$$p_S(x,0) - p_T = \frac{1}{2}\left[\sigma_T(\theta_T - \theta_B) + \sigma_B A_S - (\sigma_B - \sigma_T)A_I\right], \tag{5.8a}$$

where

$$A_S = \Delta\theta_S \ln\left\{\frac{\cosh[(\theta_T - \theta_S)/\Delta\theta_S]}{\cosh[(\theta_B - \theta_S)/\Delta\theta_S]}\right\} \tag{5.8b}$$

and

$$A_I = \Delta\theta_I \ln\left\{\frac{\cosh[(\theta_T - \theta_I)/\Delta\theta_I]}{\cosh[(\theta_B - \theta_I)/\Delta\theta_I]}\right\}. \quad (5.8c)$$

We note that $A_S \to \theta_T - 2\theta_S + \theta_B$ as $\Delta\theta_S \to 0$ and $A_I \to \theta_T - 2\theta_I + \theta_B$ as $\Delta\theta_I \to 0$. If $\sigma_T \neq \sigma_B$ then (5.8) determines the interface potential temperature θ_I (this must be computed numerically if $\Delta\theta_I > 0$); otherwise, there is no interface, and (5.8) serves as a constraint on the common value $\sigma_T = \sigma_B$.

For the initial surface potential temperature we specify

$$\theta_S(x,0) = \theta_B + \Delta\theta\left[1 + \tanh\left(\frac{x}{L}\right)\right], \quad (5.9)$$

and specify the initial surface pressure $p_S(x,0) = p_B =$ constant. Here we use the values $\sigma_B = 8\sigma_T = 2\,\text{kPa/K}$, $p_T = 5\,\text{kPa}$, $\theta_T = 400\,\text{K}$, $p_B = 100\,\text{kPa}$, $\theta_B = 265\,\text{K}$, and $\Delta\theta = 17.5\,\text{K}$. Figure 1a shows the initial (analytical) θ field as a function of x and p with $\Delta\theta_I = 5\,\text{K}$ and $\Delta\theta_S = 0\,\text{K}$; part (b) shows the corresponding initial σ^* field (5.6) as a function of X and Θ (the smoothing at the tropopause is not shown). Since $\sigma_B/(\sigma_B - \sigma_T) = 8/7$, the potential temperature variation on the tropopause is slightly larger than the potential temperature variation at the surface. According to (5.5) the two boundaries between the three σ^* regions simply steepen as frontogenesis proceeds.

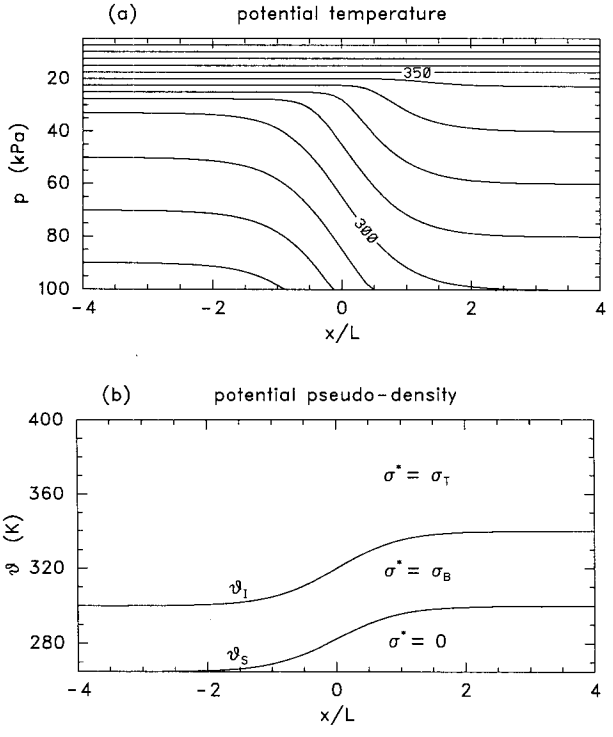

FIG. 1. (a) Initial ($\alpha t = 0$) θ field in (x,p)-space, (b) Corresponding initial σ^* field in (x,θ)-space.

The structure of the evolving front was computed at several values of αt by evaluating the potential pseudodensity σ^* analytically from (5.5) and (5.6) and then solving the invertibility relation numerically as follows. With the assumption of y independence, (3.4) reduces to a two-dimensional problem in X and Θ [cf. (5.3)], which is identical to that solved in Schubert et al. (1989) except that X is scaled by the factor $\sqrt{1+\alpha^2/f^2}$. Assuming that the deformation field is weak (i.e., $\alpha \ll f$), this factor may be dropped. We thus could use the multigrid solver described by Fulton (1989) to solve (3.4) for this frontogenesis problem. Given the distribution of σ^* specified above, the idea of a "basic state" has little meaning, so we modified the solver of Fulton (1989) to solve for M^*, rather than its deviation; the resulting numerical method is more robust, and the code is simpler. The lower boundary was taken to be flat ($\phi_S = 0$) and the top isobaric ($p = p_T$). We used a 256×32 grid covering the domain $-4 \leq X/L \leq 4$ shown in Fig. 1. At the lateral boundaries M^* was computed by assuming it to be independent of X and solving (3.4) as a boundary value problem in Θ only. For clarity, only the central portion $-1 \leq X/L \leq 1$ of the computational domain is shown in the subsequent figures.

Figure 2 shows the front at $\alpha t = 1$. Part (a) shows the potential pseudodensity σ^* evaluated on the computational grid, part (b) shows the wind (v_g) and mass (p) fields in the geostrophic/isentropic coordinates (X,Θ), and part (c) shows the wind (v_g) and mass (θ) fields in the physical coordinates (x,p). A dotted line on each figure indicates the earth's surface (θ_S or p_S). It is interesting to note that the fields in the massless layer (Fig. 2b) satisfy the assumptions given in section 4, even though these assumptions were not incorporated into the numerical solver. Corresponding results at a later time ($\alpha t = 2$) in Fig. 3 show the surface front and corresponding upper-tropospheric jet strengthening.

An interesting feature of the semigeostrophic system is that it predicts the development of a true discontinuity in finite time (Hoskins and Bretherton 1972). This result is also obtained in the isentropic coordinate formulation employed here. Figure 4 shows the computed structure of the front at $\alpha t = 3$. However, the transformation from geostrophic (X) to physical (x) coordinates has broken down at this time, so the fields shown in Fig. 4c contain some error. This is most clearly seen in Fig. 5, which shows x as a function of X;

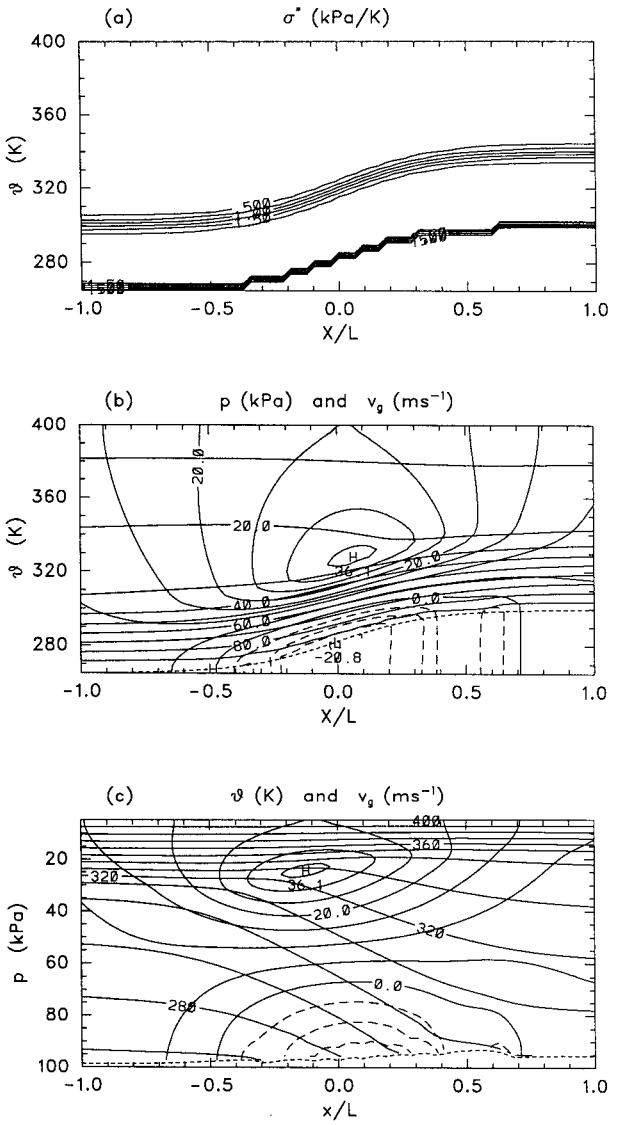

FIG. 2. Structure of the front at $\alpha t = 1$: (a) σ^* in (x, p)-space, (b) p and v_g in (X, Θ)-space, and (c) θ and v_g in (x, p)-space. Dashed contours represent $v_g < 0$ (out of the paper), and dotted lines represent the earth's surface. Note the change in the X scale from Fig. 1.

note that at the surface, θ has become a multiple-valued function of x, so in fact a true discontinuity has developed. In the real atmosphere, of course, physical processes neglected in this study (e.g., friction or Kelvin–Helmholtz instability along the front) would become significant before this time; this point is addressed in more detail in Hoskins and Bretherton (1972). Away from the surface discontinuity the computed fields at $\alpha t = 3$ should be approximately correct; we see in Fig. 6 that the model has begun to develop the folded tropopause characteristic of strong fronts in the real atmosphere (Shapiro et al. 1987). The low-level minimum of σ^* in Fig. 6 is an artifact of the coordinate transformation, which has broken down near the surface front.

6. Concluding remarks

We have shown that the most concise version of f-plane semigeostrophic theory is the version that makes simultaneous use of isentropic and geostrophic coordinates. The use of isentropic coordinates for adiabatic flow simplifies the total derivative operator to (2.6), while the use of geostrophic coordinates further simplifies the horizontal advection by making it geostrophic.

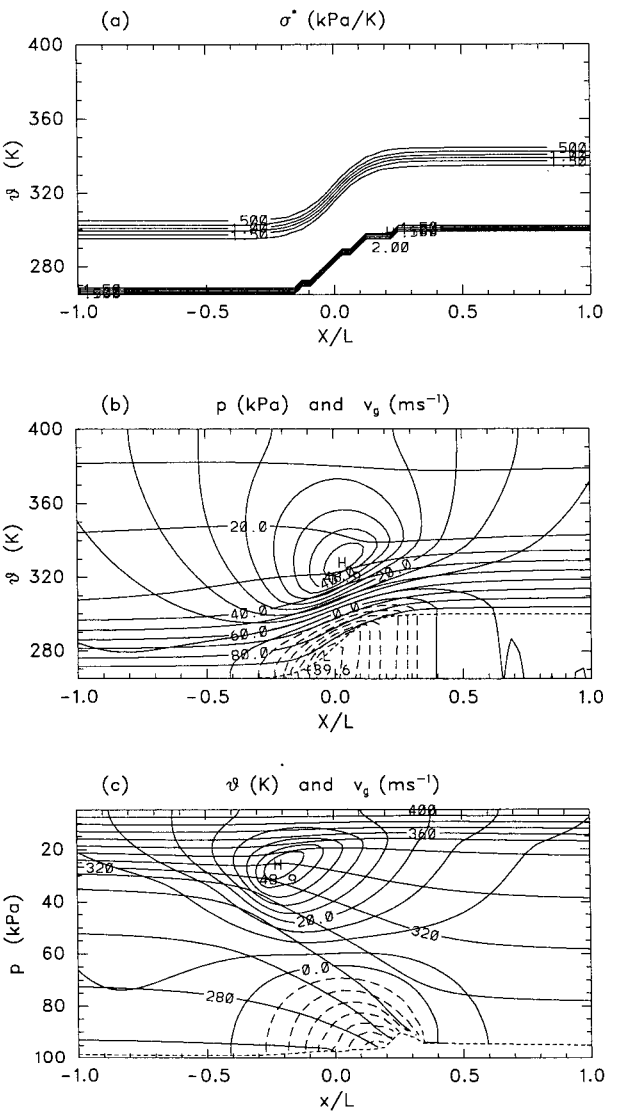

FIG. 3. Same as Fig. 2 except for $\alpha t = 2$.

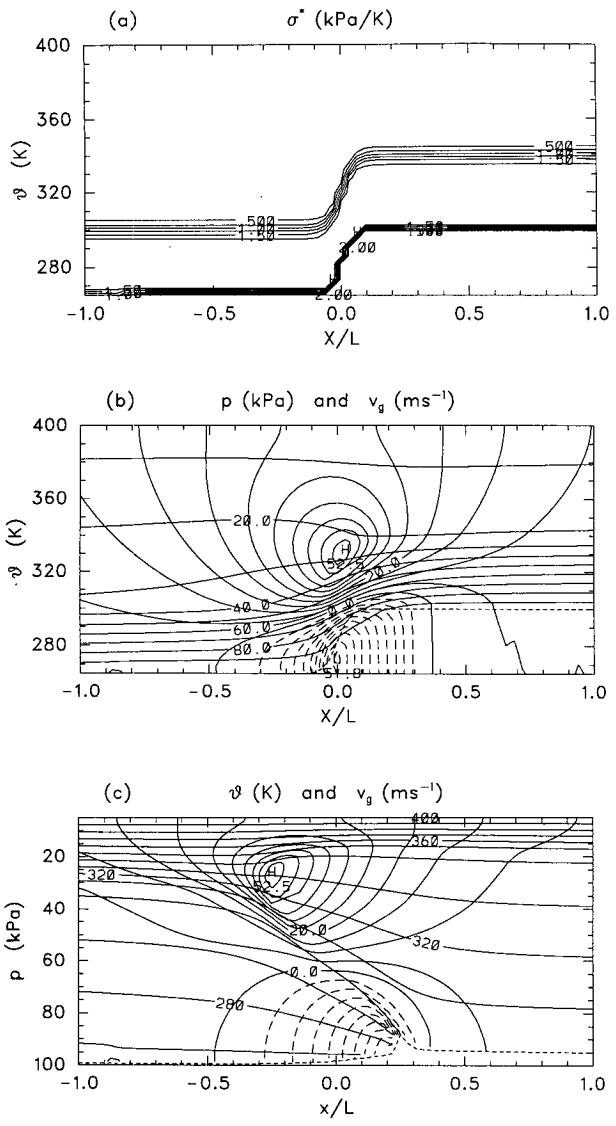

FIG. 4. Same as Fig. 2 except for $\alpha t = 3$.

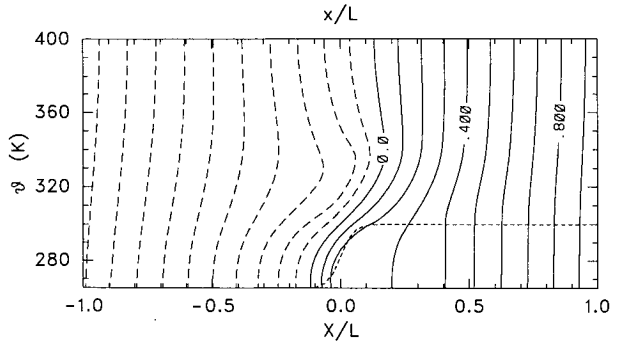

FIG. 5. Physical coordinate x/L in (X, Θ)-space at $\alpha t = 3$.

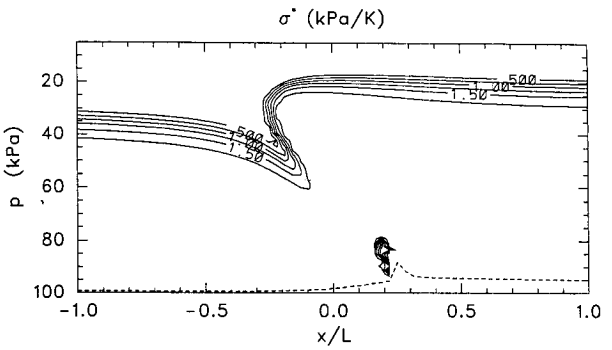

FIG. 6. Potential pseudodensity (inverse potential vorticity) σ^* in (x, p)-space at $\alpha t = 3$.

The fundamental predictive equation for potential pseudodensity then takes the simple form (2.11), and the invertibility principle (3.4) closes the theory. This basic structure of a closed theory based on a predictive equation for σ^* and an invertibility principle for M^* is maintained in the β plane and hemispheric generalizations of semigeostrophic theory presented by Magnusdottir and Schubert (1990, 1991). The combined use of isentropic and generalized geostrophic coordinates is crucial for the mathematical simplicity of these β-plane and hemispheric semigeostrophic theories. The recurring importance of isentropic coordinates in the simplicity of all these theories emphasizes the need to develop techniques for handling situations in which isentropes intersect the ground. Here we have investigated the massless layer approach to this problem. By extending the validity of the invertibility condition into the massless layer we have shown that the classic surface frontogenesis problem can be handled in a computationally convenient and accurate way that is consistent with IPV thinking. These results should remove one of the commonly heard criticisms of isentropic coordinates and hopefully widen the scope of problems to which IPV modeling can be applied.

Acknowledgments. This work was supported by the National Science Foundation, under Grants ATM-8814541 and ATM-8918725, and the Office of Naval Research, under Grant N000014-88-K-0214.

APPENDIX

Validity of the Hydrostatic Relation at $\theta = \theta_S$

In section 4 we showed how to extend M and Π to the massless layer $\theta < \theta_S$ so that both variables are continuous at $\theta = \theta_S$ and the hydrostatic relation

$$\frac{\partial M}{\partial \theta} = \Pi \tag{A1}$$

holds for $\theta > \theta_S$ and for $\theta < \theta_S$. The fact that (A1) also holds at $\theta = \theta_S$ is a consequence of the Removable Singularity Theorem and may be proven directly as follows. By the Mean Value Theorem, for any $\theta_1 > \theta_S$, there exists a $\hat{\theta}_1$ with $\theta_S < \hat{\theta}_1 < \theta_1$ such that

$$\frac{M(\theta_1) - M(\theta_S)}{\theta_1 - \theta_S} = \left.\frac{\partial M}{\partial \theta}\right|_{\theta=\hat{\theta}_1} = \Pi(\hat{\theta}_1). \tag{A2}$$

Thus,

$$\lim_{\theta_1 \to \theta_S +} \frac{M(\theta_1) - M(\theta_S)}{\theta_1 - \theta_S} = \lim_{\theta_1 \to \theta_S +} \Pi(\hat{\theta}_1) = \Pi(\theta_S) \tag{A3}$$

by the continuity of Π at θ_S. An analogous argument for $\theta_2 < \theta_S$ shows that

$$\lim_{\theta_2 \to \theta_S -} \frac{M(\theta_S) - M(\theta_2)}{\theta_S - \theta_2} = \Pi(\theta_S). \tag{A4}$$

From (A3) and (A4), both one-sided derivatives of M exist at $\theta = \theta_S$ and are equal to $\Pi(\theta_S)$, so in fact M is differentiable at $\theta = \theta_S$ and (A1) holds there.

REFERENCES

Arakawa, A., and Y.-J. Hsu, 1990: Energy conserving and potential-enstrophy dissipating schemes for the shallow water equations. *Mon. Wea. Rev.*, **118**, 1960–1969.

Andrews, D. G., 1983: A finite-amplitude Eliassen-Palm theorem in isentropic coordinates. *J. Atmos. Sci.*, **40**, 1877–1883.

Bretherton, F. P., 1966: Critical layer instability in baroclinic flows. *Quart. J. Roy. Meteor. Soc.*, **92**, 325–334.

Buzzi, A., A. Trevisan, and G. Salustri, 1981: Internal frontogenesis: A two-dimensional model in isentropic, semigeostrophic coordinates. *Mon. Wea. Rev.*, **109**, 1053–1060.

Eliassen, A., 1948: The quasi-static equations of motion. *Geofys. Publ.*, **17**(3), 1–44.

Ertel, H., 1942: Ein neuer hydrodynamischer Wirbelsatz. *Meteorologische Zeitschrift*, **59**, 277–281. [English translation available from W. Schubert, Dept. of Atmos. Sci., Colorado State University, Fort Collins, CO 80523.]

Fulton, S. R., 1989: Multigrid solution of the semigeostrophic invertibility relation. *Mon. Wea. Rev.*, **117**, 2059–2066.

Hoskins, B. J., 1971: Atmospheric frontogenesis: Some solutions. *Quart. J. Roy. Meteor. Soc.*, **97**, 139–153.

——, 1972: Non-Boussinesq effects and further development in a model of upper tropospheric frontogenesis. *Quart. J. Roy. Meteor. Soc.*, **98**, 532–541.

——, B. J., 1975: The geostrophic momentum approximation and the semigeostrophic equations. *J. Atmos. Sci.*, **32**, 233–242.

——, and F. P. Bretherton, 1972: Atmospheric frontogenesis models: Mathematical formulation and solution. *J. Atmos. Sci.*, **29**, 11–37.

——, M. E. McIntyre, and A. W. Robertson, 1985: On the use and significance of isentropic potential vorticity maps. *Quart. J. Roy. Meteor. Soc.*, **111**, 877–946.

Hsu, Y.-J., and A. Arakawa, 1990: Numerical modeling of the atmosphere with an isentropic vertical coordinate. *Mon. Wea. Rev.*, **118**, 1933–1959.

James, I. N., and B. J. Hoskins, 1985: Some comparisons of atmospheric internal and boundary baroclinic instability. *J. Atmos. Sci.*, **42**, 2142–2155.

Lorenz, E. N., 1955: Available potential energy and the maintenance of the general circulation. *Tellus*, **7**, 157–167.

Magnusdottir, G., and W. H. Schubert, 1990: The generalization of semi-geostrophic theory to the β-plane. *J. Atmos. Sci.*, **47**, 1714–1720.

——, and W. H. Schubert, 1991: Semigeostrophic theory on the hemisphere. *J. Atmos. Sci.*, **48**, 1449–1456.

McWilliams, J. C., and P. R. Gent, 1980: Intermediate models of planetary circulations in the atmosphere and ocean. *J. Atmos. Sci.*, **37**, 1657–1678.

Montgomery, R. B., 1937: A suggested method for representing gradient flow in isentropic surfaces. *Bull. Amer. Meteor. Soc.*, **18**, 210–212.

Rossby, C.-G., 1937: Isentropic analysis. *Bull. Amer. Meteor. Soc.*, **18**, 201–209.

——, 1940: Planetary flow patterns in the atmosphere. *Quart. J. Roy. Meteor. Soc.*, **66**(Suppl), 68–87.

Schubert, W. H., and B. T. Alworth, 1987: Evolution of potential vorticity in tropical cyclones. *Quart. J. Roy. Meteor. Soc.*, **113**, 147–162.

——, S. R. Fulton, and R. F. A. Hertenstein, 1989: Balanced atmospheric response to squall lines. *J. Atmos. Sci.*, **46**, 2478–2483.

——, P. E. Ciesielski, D. E. Stevens, and H.-C. Kuo, 1991: Potential vorticity modeling of the ITCZ and the Hadley circulation. *J. Atmos. Sci.*, **48**, 1493–1509.

Shapiro, M. A., T. Hampel, and A. J. Krueger, 1987: The arctic tropopause fold. *Mon. Wea. Rev.*, **115**, 444–454.